Supplementary Material

Operando μ-Raman Measurement of the Water Distribution Along and Across the Membrane in the Fuel Cell

Thi B. H. Tran[1,*], Patrice Huguet[1], Arnaud Morin[2], Mike Robitzer[3], Stefano Deabate[1,z]

[1]IEM, Univ Montpellier, ENSCM, CNRS, Montpellier, France
[2]Université Grenoble Alpes, CEA-Liten, Grenoble F-38000, France
[3]ICGM, Univ Montpellier, ENSCM, CNRS, Montpellier, France

[*]Present address: Université Grenoble Alpes, CEA-Liten, Grenoble F-38000, France

[z]E-mail: stefano.deabate@umontpellier.fr

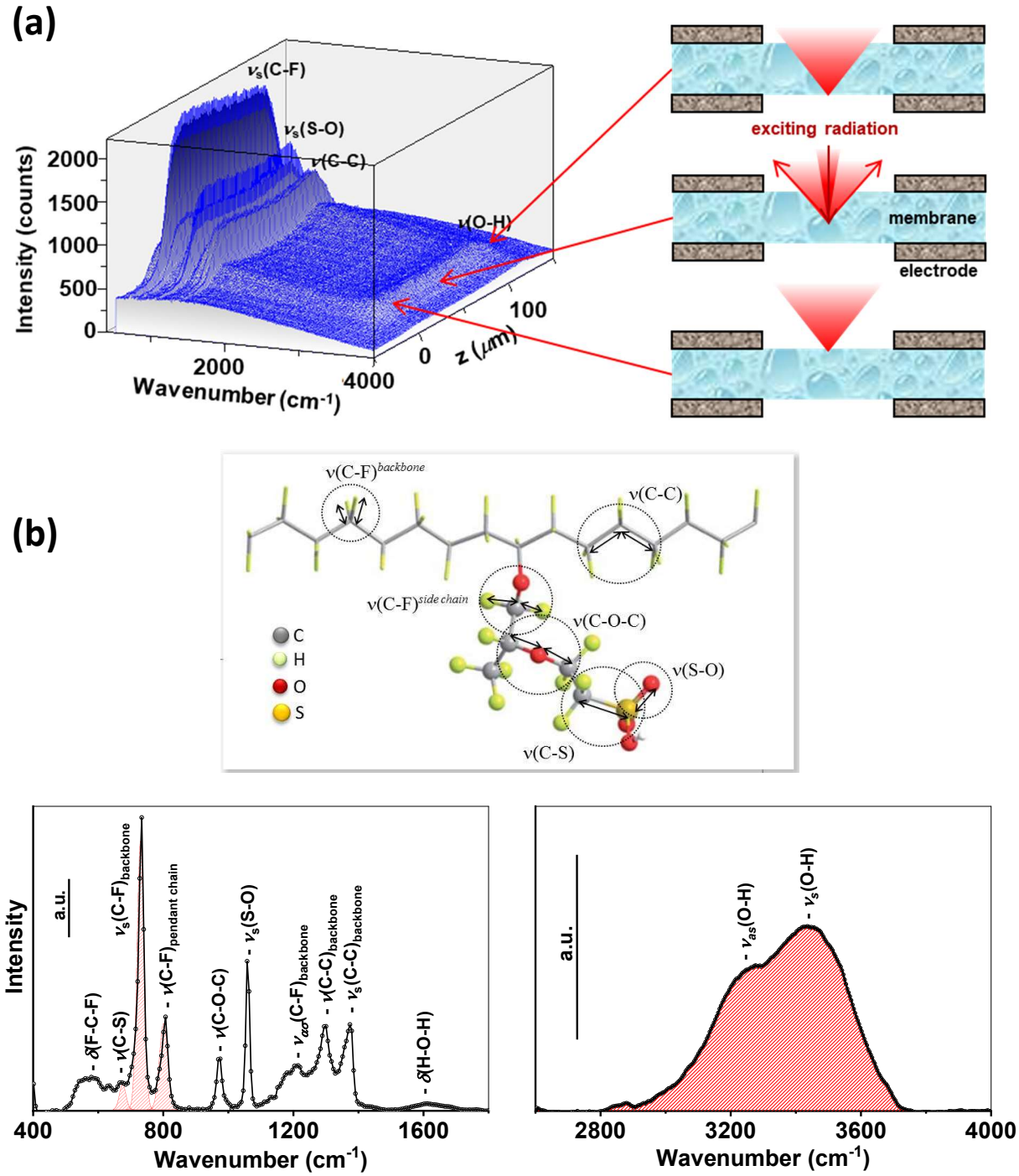

Figure S1. Schematic illustration of the basis of μ-Raman measurement of water sorbed in the membrane. (a) 3-D view of the Raman signal intensity evolution across the membrane in the model FC under homogeneous conditions: OCV and RH = 90% at both FC sides. (b) Raman spectra of the Nafion® N115 membrane soaked in water at T_{room} during 2h (λ = 13). Top: schematic representation of the local Nafion® structure with main vibrational modes. Left: wavenumber range of bands arising from vibrations of molecular groups belonging to the polymer phase and δ(H-O-H) mode. Right: ν(O-H) modes from sorbed water. Spectral attributions are according to Peng et al..[1] The integrated signals of water and fluorinated matrix used to assess the membrane water content are indicated in red.

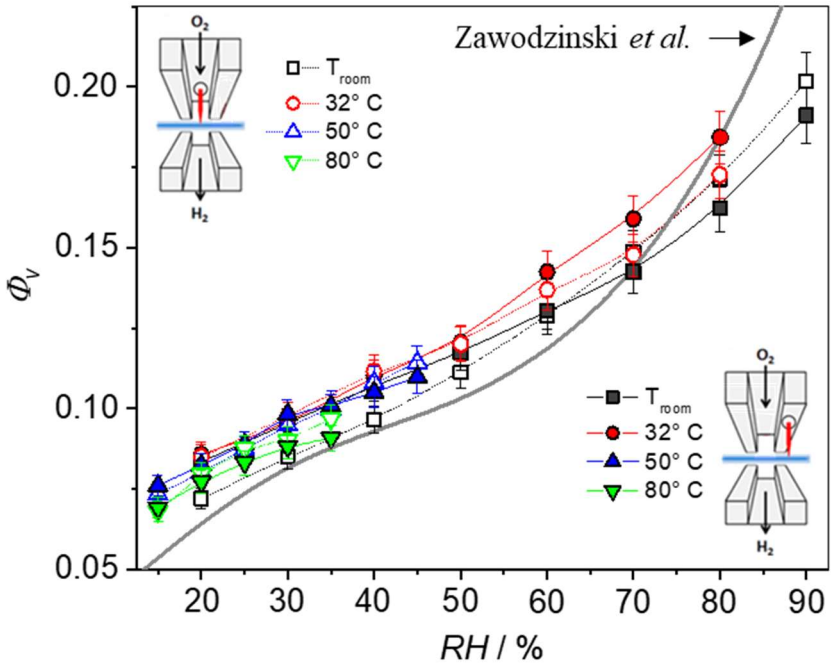

Figure S2. Comparison between the Nafion® N115 sorption isotherms obtained by μ-Raman measurement in the model FC (symbols) and by gravimetric measurements (at T_{room} as reported by Zawodzinski et al.,[2] grey line). Full symbols correspond to the membrane area under the lands for current collection and open symbols to the channel for the feed gas distribution. Errors in the RH measurements are inside the symbol size.

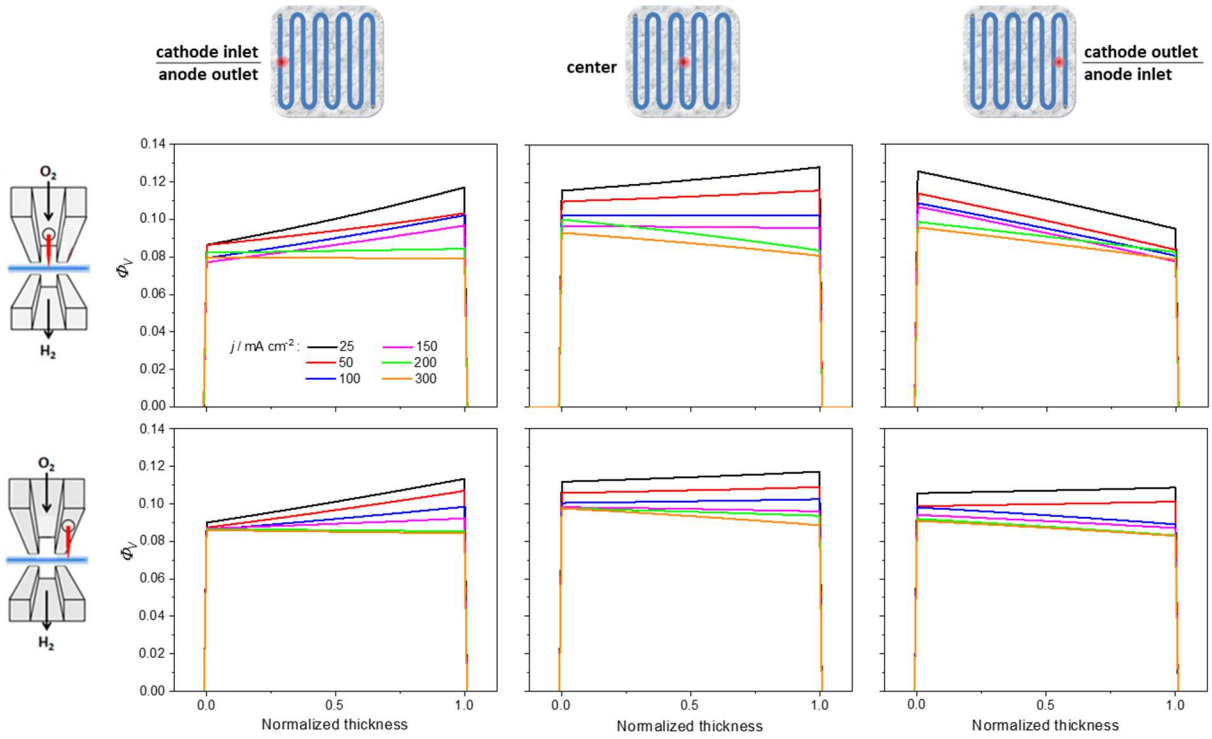

Figure S3. Comparison of the evolution of the membrane inner water distribution with the current density (reported in the legend) at the different probed positions (top: channel, bottom: lands, left: cathode inlet, middle: center, right: cathode outlet) in the cell operated at 32°C.

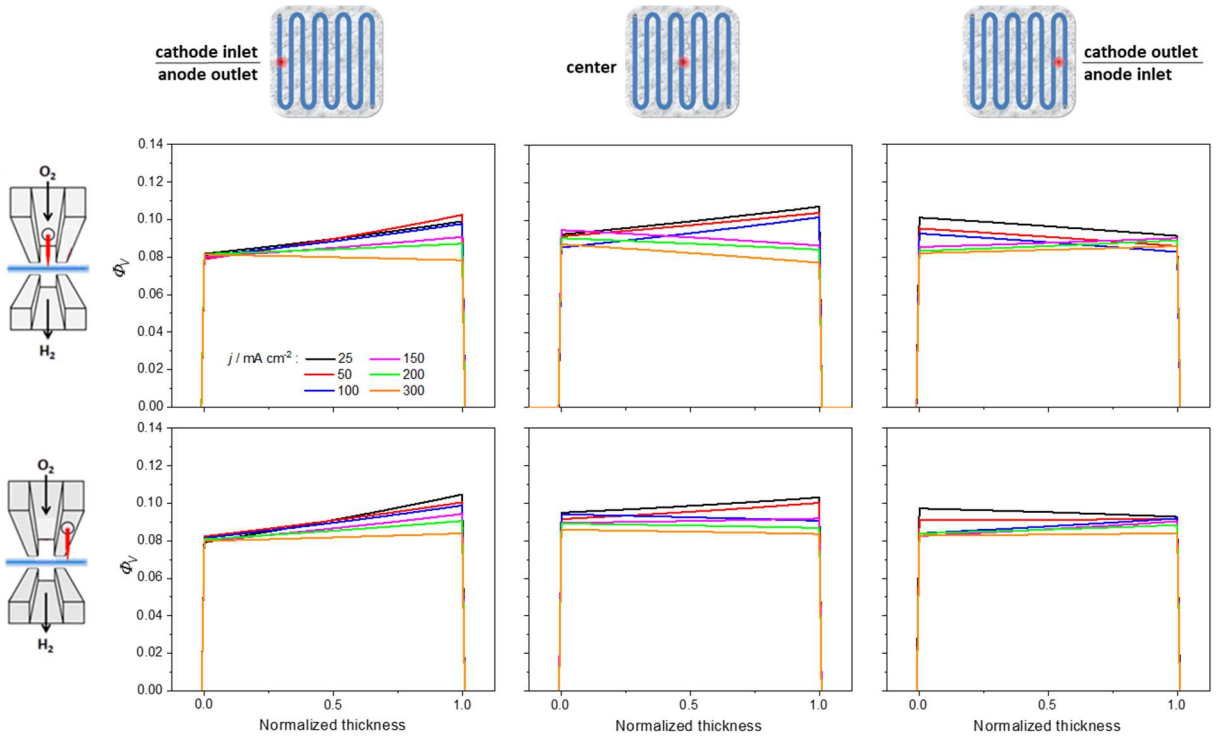

Figure S4. Comparison of the evolution of the membrane inner water distribution with the current density (reported in the legend) at the different probed positions (top: channel, bottom: lands, left: cathode inlet, middle: center, right: cathode outlet) in the cell operated at 50°C.

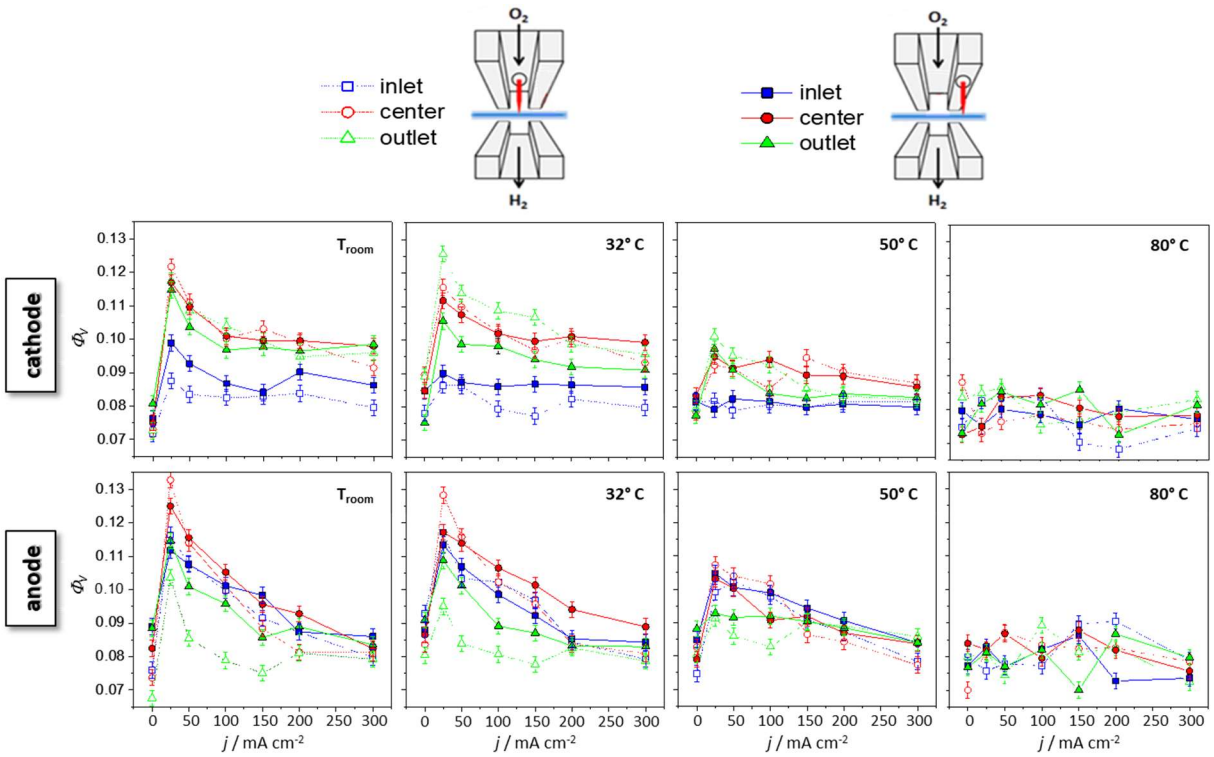

Figure S5. Comparison of the evolution with the current density of the membrane water volume fraction at the cathode (top) and anode (bottom) surfaces, at the channel (open symbols) and under-lands (full symbols) positions, in the cell operated at different *T*.

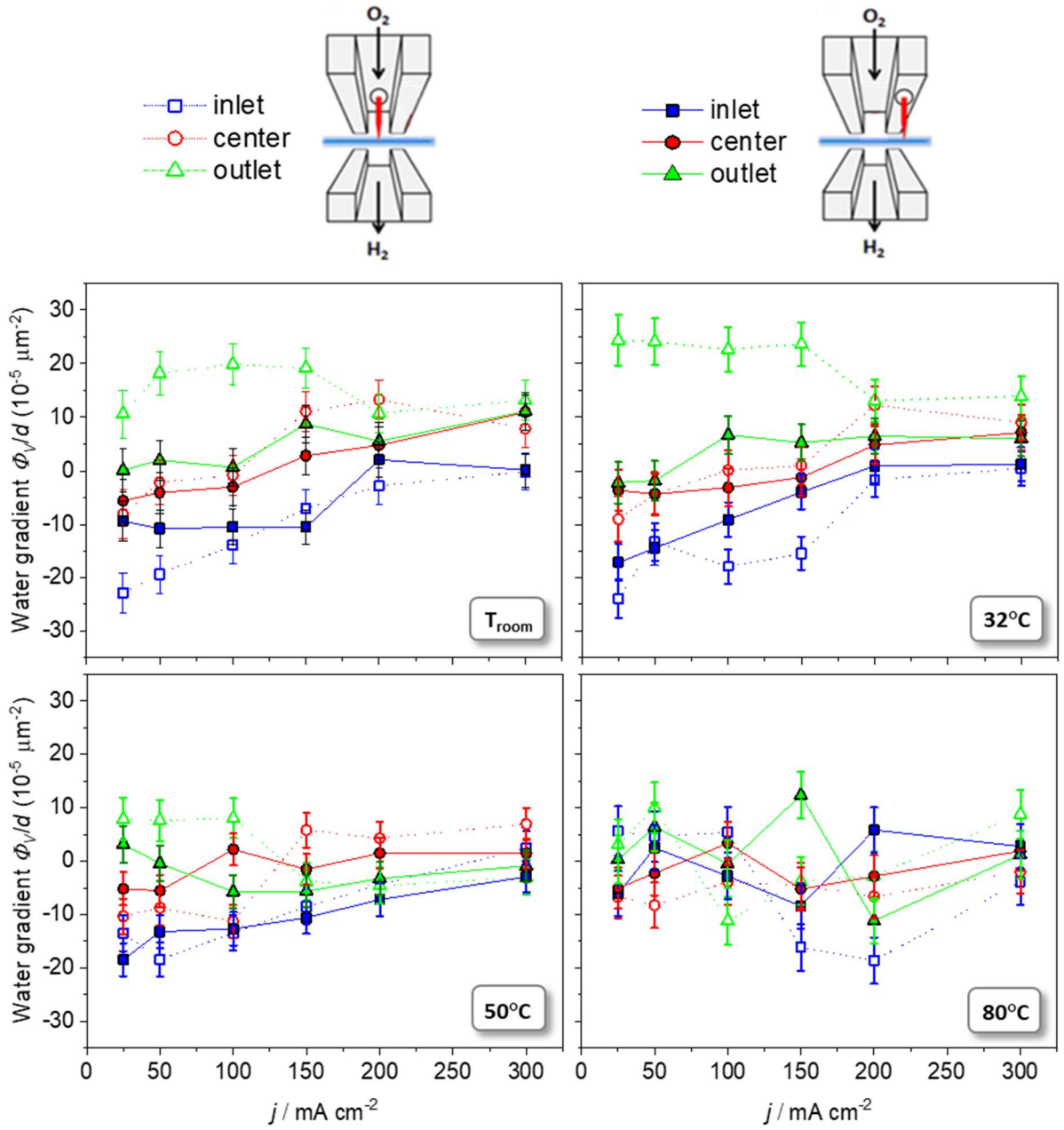

Figure S6. Evolutions with the current density of the membrane inner water gradient $\Delta\Phi_V$ / d (where $\Delta\Phi_V = \Phi_{V\,/\,cathode} - \Phi_{V\,/\,anode}$) at the channel and under-lands areas of the cell operated at different T (corresponding d are reported in Figure S7).

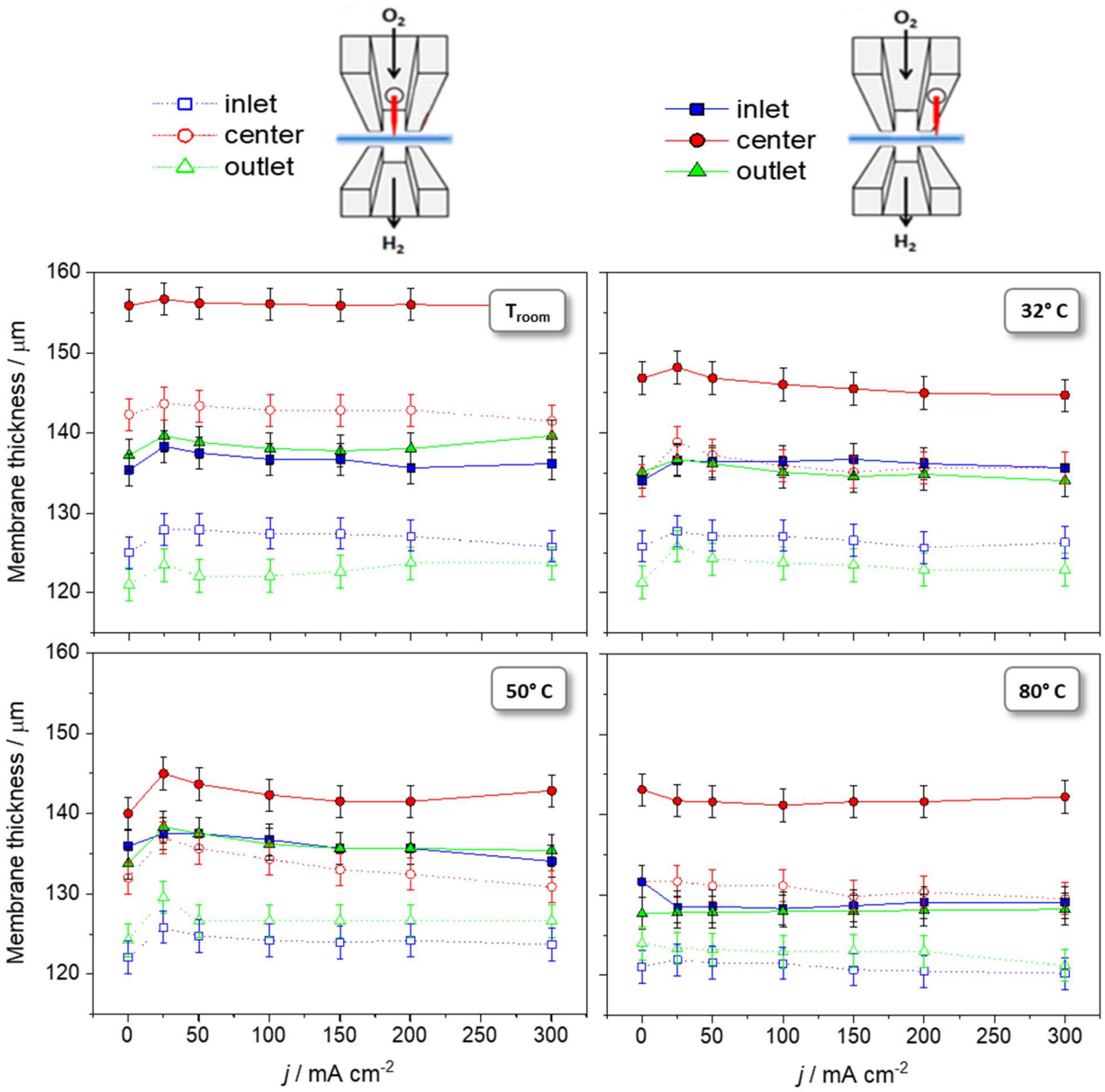

Figure S7. Evolution with the current density of the membrane thickness at the channel (open symbols) and under-lands (full symbols) positions in the cell operated at different *T*.

1. Z. Peng, P. Huguet, S. Deabat, A. Morin and A.-K. Sutor, *J. Raman Spectrosc.*, **44**, 321 (2013).

2. T. A. Zawodzinski, C. Derouin, S. Radzinski, R. J. Sherman, V. T. Smith, T. E. Springer and S. Gottesfeld, *J. Electrochem. Soc.*, **140**, 1041 (1993).